PASSIVE IN-BAND RF POWER SENSING IN THIN-FILM LITHIUM NIOBATE ON SILICON PLATFORM

Hakhamanesh Mansoorzare and Reza Abdolvand
University of Central Florida, USA

2024 IEEE 37th International Conference on Micro Electro Mechanical Systems (MEMS) | 979-8-3503-5792-9/24/$31.00 ©2024 IEEE | DOI: 10.1109/MEMS58180.2024.10439505

ABSTRACT

A frequency selective and passive method for RF power sensing is reported that leverages the interaction of guided Lamb waves and electrons in thin-film lithium niobate (LN) on silicon (Si). The incoming RF signal is first transduced into Lamb waves via the piezoelectricity of LN and is then converted into an electron flow in the Si. The generated direct current (DC) is proportional to the RF power and appears only within the passband frequency of the waveguide which is defined lithographically by the interdigital transducers (IDT) lateral dimensions. Preliminary results show at least 30 dB dynamic range and faster than 1 ms response time. The reported dynamic range is believed to be far from the full potential of this scheme and could be improved by design/optimization, thus, enabling realization of integrated power sensors in micro-acoustic domain.

KEYWORDS

Acoustoelectric, Lamb wave, lithium niobate, micro-acoustic, piezoelectric, RF power sensing, waveguide.

INTRODUCTION

Radio frequency (RF) power measurement is critical in telecommunications for increasing power and spectrum efficiency. Currently, heat- or diode-based solutions are commonly used for power sensing. The former, including thermistors and thermocouples, do so by dissipating RF power and measuring the temperature increase within a resistive termination, offering some advantages in terms of accuracy, linearity, and stability but at the cost of few to tens of ms response time. The latter, on the other hand, uses rectification of the voltage across the resistive termination, offering fast response time, wide dynamic range, and highest degree of compatibility with different scenarios and applications [1]. The main drawbacks of diode-based solutions are high temperature induced drift of output and cost considerations regarding power consumption, matching, and chip area at gigahertz range [2].

Since the piezoelectric platform is ubiquitous in RF communication devices for signal processing, its application in power sensing is quite attractive considering the module size, cost, and complexity reduction prospects. It has been known that acoustic waves in piezoelectric media are accompanied by a piezoelectric potential wave that can interact with electrons, drag them, and generate a direct current (DC) known as the acoustoelectric (AE) current [3]. Consequently, numerous works have used this property in surface acoustic wave (SAW) platform for niche applications such as metrology, quantum processing, probing electronic properties of 2D material, photo-detection, and solar cells, to name a few [4]-[7]. Nearly all these efforts have been based on ultra-thin or 2D semiconductors on piezoelectric substrates, as they minimally perturb the SAW and allow for exploiting the moderate piezoelectric coupling achievable on such substrates. More recently, owing to the progress in thin-film transfer and growth, strong AE interactions have been attained in thin-film piezoelectric platform, resulting in record low-power and miniaturized traveling wave amplifiers [8]-[10]. Inspired by the strong energy coupling between Lamb waves and electrons in thin-film lithium niobate (LN)-on-silicon (Si) [8] and the bright outlook of suspended LN micro-acoustics [11], in this work we explore the potential of AE effect for frequency selective RF power detection and sensing.

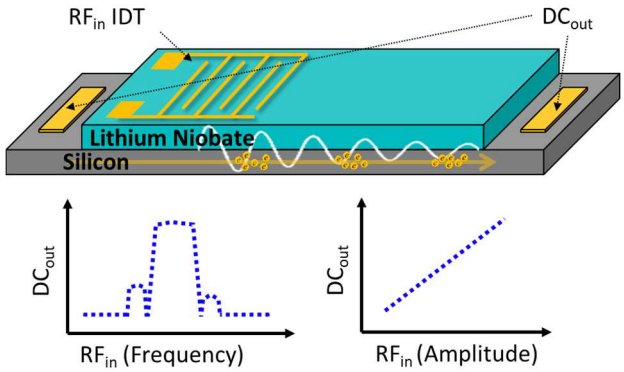

Figure 1: Conceptual schematic of RF-to-DC conversion in Lamb mode lithium niobate on silicon waveguides. The generated DC output appears mainly within the passband of the waveguide and is proportional to the Lamb wave (and input RF signal) amplitude.

OPERATING PRINCIPLE

The conceptual schematic of the RF-to-DC conversion in a LN-on-Si waveguide is shown in Fig. 1. The input RF signal is transduced into traveling Lamb waves via the input interdigital transducer (IDT) formed on the LN surface. The IDT design would determine the center frequency and bandwidth of Lamb waves which subsequently propagate within the waveguide, dragging along electrons in Si, and generating a DC which can be measured across the waveguide via contacts to Si, in the form of a short circuit current or an open circuit voltage. The magnitude of the AE current density (J) is in the form of

$$J = S(\alpha\mu/v) \quad (1),$$

with S being the acoustic wave intensity, α being the phonon-electron loss (see [8]), μ being the electron mobility, and v being the acoustic wave velocity. As long as the Lamb wave intensity is linear with respect to the input RF power and both the electron mobility to acoustic velocity ratio and the phonon-electron coupling are constant, the relationship between the generated DC and

the input RF power remains linear. Since deviations from said conditions often occur at higher levels of RF power, the dynamic range is more likely to be limited at the higher RF power range.

To increase the RF-to-DC conversion efficiency, it is crucial for the phonon-electron coupling (α) to be maximized; this is achieved in this work using 1 µm X-cut Y30 LN on 1 µm lightly n-type doped Si to form the waveguide and targeting fundamental symmetric (S0) mode. The COMSOL simulated stress profile of S0 mode within the waveguide is shown in Fig. 2. The cross-sectional stress profile shown within an acoustic wavelength also highlights the electric field extending beyond the LN layer.

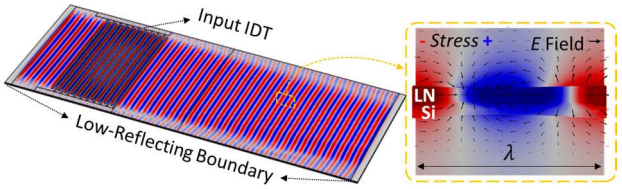

Figure 2: Finite element simulation showing Lamb wave propagation within the micromachined waveguide and its cross-sectional stress profile within a wavelength. The propagating piezoelectric field captures and drags electrons, generating a direct current.

RESULTS AND DISCUSSION

As a proof-of-concept, 2-port waveguides reported in [8] are used in this work to explore the AE RF-to-DC conversion effect. The input RF signal (in the form of a sinusoidal continuous wave produced by a signal generator) is fed into one port while the other port is left floating (terminated by a high impedance). The generated DC (short circuit current or open circuit voltage) is recorded by connecting the Si contact points to a digital multimeter as the input RF power and frequency are swept. The input RF port reflection of the waveguide is shown in Fig. 3 (blue curve). The S0 mode dip around ~610 MHz is evident and coincides with the frequencies at which the generated DC is mainly observed (red points). The scanning electron micrograph (SEM) of the 2-port LN-on-Si waveguide under test is shown in the inset of Fig. 3.

Additionally, the RF-to-DC conversion curve, shown in Fig. 3, remains linear within at least 30 dB of input power range. It is worth noting that the lowest reported measured RF power (-20 dBm) falls at the DC readout detection limit (~5 nA), therefore, the dynamic range is expected to be greater than 30 dB. In order to estimate the response time for RF-to-DC conversion, the input RF source and the output DC contacts are connected to an oscilloscope. Fig. 4 shows typical measured time-domain waveforms from which the response time is estimated to be less than 1 ms; this is shown as the time difference between the moment the ~610 MHz input at 6 dBm is turned on (green curve) and the moment the DC level is stabilized at ~4 V (yellow curve).

The performance obtained in proof-of-concept waveguides is far from optimal, especially in terms of dynamic range and sensitivity. The energy losses due to the bidirectionality of IDT and its mismatch to 50 Ω (180-j30 Ω in this case) and the acoustic reflection at the end of the waveguide, the geometry of which has yet to be optimized, are immediate limiting factors that could be addressed in future works. The proposed solution, though offering a lower dynamic range relative to diode-based counterparts, is fully passive and compared to thermal-based power sensing solutions offers a faster response time. What makes this scheme unique is the frequency selective nature of the RF-to-DC conversion which can be beneficial for reducing noise and interference. The IDT periodicity and the number of its unit cells determine the passband frequency and bandwidth of the RF-to-DC conversion while its aperture along with the number of its unit cells could be used to obtain a 50 Ω termination which is crucial for minimizing the power measurement error in most RF systems.

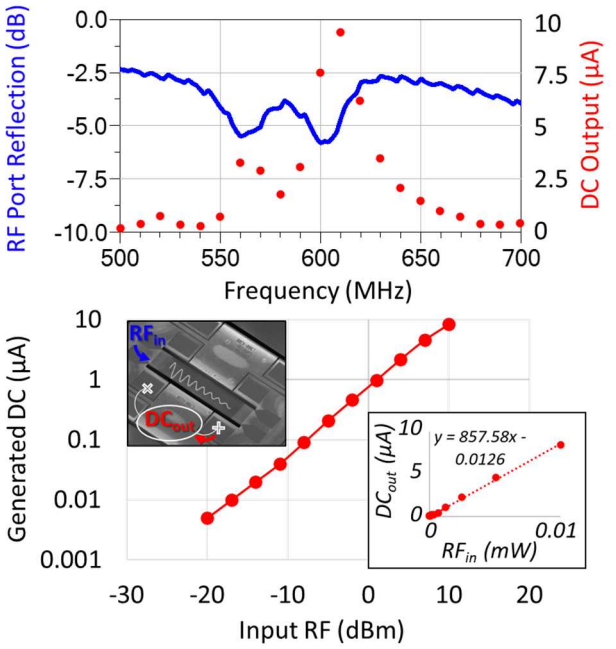

Figure 3: (top) Measured RF reflection at the input RF port of the device (blue) along with the DC output (red) generated mainly within its passband. (bottom) RF-to-DC conversion curve at ~610 MHz showing a linear response across at least 30 dB of input RF power range (-20 dBm to 10 dBm).

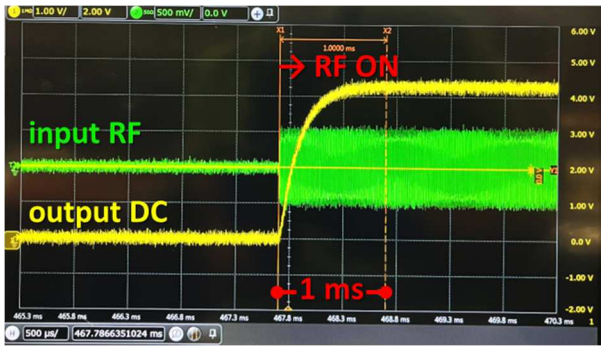

Figure 4: The output DC level (yellow) is stabilized within 1 ms of switching ON the input RF signal (green). Here ~4 V output DC is measured for an input RF at 6 dBm.

ACKNOWLEDGEMENTS

The authors would like to thank NGK Insulators for providing bonded LN on SOI substrates. This work was supported by the National Science Foundation under Grant 2122670.

REFERENCES

[1] A. S. Brush, "Measurement of microwave power-A review of techniques used for measurement of high-frequency RF power." *IEEE instrumentation & measurement magazine* 10.2 (2007): 20-25.

[2] J. G. Ravanne, Y. L. Then, H. T. Su, and I. Hijazin, "Microwave Power Detectors in Different CMOS Design Architectures: A Review." *IEEE Microwave Magazine* 23.6 (2022): 76-84.

[3] X. Nie, et al. "Surface acoustic wave induced phenomena in two-dimensional materials." *Nanoscale Horizons* 8.2 (2023): 158-175.

[4] T. Poole and G. R. Nash, "Acoustoelectric current in graphene nanoribbons." *Scientific Reports* 7.1 (2017): 1767.

[5] A. D. Barros, P. D. Batista, A. Tahraoui, J. A. Diniz, and P. V. Santos, "Ambipolar acoustic transport in silicon." *Journal of Applied Physics* 112.1 (2012).

[6] V. Miseikis, J. E. Cunningham, K. Saeed, R. O'Rorke, and A. G. Davies, "Acoustically induced current flow in graphene." *Applied Physics Letters* 100.13 (2012).

[7] A. R. Rezk, et al. "Acoustically-driven trion and exciton modulation in piezoelectric two-dimensional MoS2." *Nano letters* 16.2 (2016): 849-855.

[8] H. Mansoorzare and R. Abdolvand, "Micromachined Heterostructured Lamb Mode Waveguides for Acoustoelectric Signal Processing", *IEEE Transactions on Microwave Theory and Techniques* 70.11 (2022): 5195-5204.

[9] L. Hackett, et al. "Non-reciprocal acoustoelectric microwave amplifiers with net gain and low noise in continuous operation." Nature Electronics 6.1 (2023): 76-85.

[10] L. Hackett, et al. "S-band acoustoelectric amplifier utilizing an ultra-high thermal conductivity heterostructure for low self-heating." arXiv preprint arXiv:2309.15725 (2023).

[11] R. Lu and S. Gong, "RF acoustic microsystems based on suspended lithium niobate thin films: Advances and outlook." Journal of Micromechanics and Microengineering 31.11 (2021): 114001.

CONTACT

*H. Mansoorzare, tel: +1-352-3464400;
hakha@ucf.edu